A&A 456, 1181–1185 (2006)
DOI: 10.1051/0004-6361:20065212

Astronomy & Astrophysics

New and improved experimental oscillator strengths in Zr II and the solar abundance of zirconium*

G. Ljung[1], H. Nilsson[1], M. Asplund[2], and S. Johansson[1]

[1] Atomic Astrophysics, Lund Observatory, Box 43, 221 00 Lund, Sweden
[2] Research School of Astronomy and Astrophysics, Australian National University, Mt. Stromlo Observatory, Cotter Rd., Weston, ACT 2611, Australia

Received 15 March 2006 / Accepted 19 June 2006

ABSTRACT

Using the Fourier Transform Spectrometer at Lund Observatory, intensity calibrated spectra of singly ionized zirconium have been recorded and analyzed. Oscillator strengths for 263 Zr II spectral lines in the region 2500–5400 Å have been derived by combining new experimental branching fractions with previously measured radiative lifetimes. The transitions combine 34 odd parity levels with 29 low metastable levels between 0 and 2.4 eV. The experimental branching fractions have been compared with theoretical values and the oscillator strengths with previously published data when available. The oscillator strengths have been employed to derive the solar photospheric Zr abundance based on both 1D and 3D model atmospheres. Based on the seven best and least perturbed Zr II lines in the solar disk-center spectrum, we determine the solar Zr abundance to $\log \varepsilon_{\rm Zr} = 2.58 \pm 0.02$ when using a 3D hydrodynamical solar model atmosphere. The new value is in excellent agreement with the meteoritic Zr abundance.

Key words. atomic data – line: identification – methods: laboratory – Sun: abundances

1. Introduction

In chemical analyses of cosmic plasmas, such as stellar atmospheres, nebulae and the interstellar medium, there is a need for accurate experimental values of atomic parameters, e.g. wavelengths, oscillator strengths and energy levels. The chemical analysis of a stellar atmosphere involves the determination of elemental abundances, where some elements may be of more importance than others. One such example is zirconium, since it is a member of the Sr-Y-Zr triad and therefore important for studies of the s-process nucleosynthesis (e.g. Busso et al. 1999). The zirconium abundance can be measured from stellar absorption lines provided that the inherent line strength, the oscillator strength (f-value), is known. For example, the solar zirconium abundance has been determined from Zr I and Zr II lines (e.g. Biémont et al. 1981). Zirconium is overabundant in the HgMn star χ Lupi but the abundances derived from Zr II and Zr III lines do not agree (Sikström et al. 1999).

Previous experimental determinations of oscillator strengths for 321 lines in Zr II have been made by Corliss & Bozman (1962) using an arc as a light source. Biémont et al. (1981) reported oscillator strengths for 31 lines using branching fractions and lifetimes. Bogdanovich et al. (1995) calculated oscillator strengths for 15 Zr II lines using the superposition-of-configurations method. Malcheva et al. (2006) reported transition probabilities for 243 transitions combining experimental data with relativistic Hartree-Fock calculations including core-polarization. In this paper we present oscillator strengths for 263 Zr II lines in the spectral range 2500 to 5400 Å. From line intensities measured with the Lund Fourier Transform Spectrometer (FTS), we have derived branching fractions (BFs), which are combined with lifetimes from laser induced fluorescence measurements by Biémont et al. (1981), Langhans et al. (1995) and Sikström et al. (1999). The line intensities are calibrated for the instrument response and corrected for self-absorption. The contribution from lines not possible to measure is calculated with the Cowan (1981) code.

The solar abundance of zirconium has been investigated by for example Biémont et al. (1981), Gratton & Sneden (1994) and Bogdanovich et al. (1995). Biémont et al. found a value of $\log \varepsilon_{\rm Zr} = 2.56 \pm 0.05$ using 34 Zr I and 24 Zr II lines, which Gratton & Sneden revised by using a different 1D solar model atmosphere while adopting the same input line data. Bogdanovich et al. derived a value of $\log \varepsilon_{\rm Zr} = 2.60 \pm 0.06$ using 21 Zr I and 15 Zr II lines using new theoretical oscillator strengths. These studies have relied on measured equivalent widths to derive the Zr abundances. In all cases the quoted errors are twice the error of the mean value, while the line-to-line scatter is substantial, implying large uncertainties in the transition probabilities. The solar Zr abundance ($\log \varepsilon_{\rm Zr} = 2.59 \pm 0.04$) adopted in the compilations of Lodders (2003) and Asplund et al. (2005a) stems from the Zr I result of Gratton & Sneden. In the present study, we perform a new analysis of the solar Zr abundance using our improved laboratory transition probabilities of Zr II while selecting only the best solar features. For the purpose, we have employed both a time-dependent, 3D hydrodynamical model of the solar atmosphere (Asplund et al. 2000a) as well as two standard 1D hydrostatic models: the Holweger & Müller (1974) semi-empirical and the MARCS (Gustafsson et al. 1975; Asplund et al. 1997) theoretical models.

2. The Zr II spectrum

Zr II is a complex spectrum because its configurations are based on multiple series limits. The next higher ion Zr III has three low

---

* Tables 2 and 3 are only available in electronic form at `http://www.edpsciences.org`

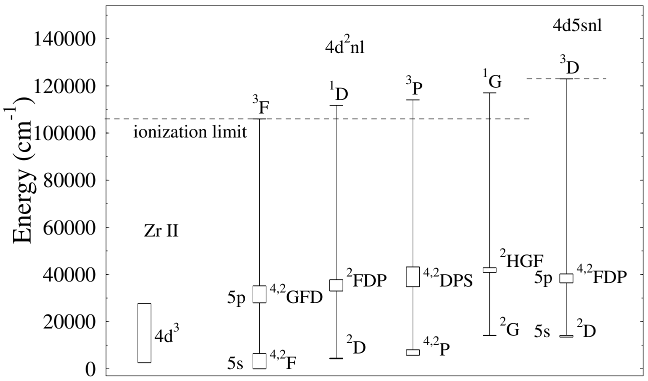

Fig. 1. Partial term diagram of Zr II. Each box represents all levels belonging to the same subconfiguration, i.e. based on the same parent term (e.g. 4d^2(^{3}P)5s ^{4}P and ^{2}P, 4d5s(^{3}D)5p ^{4}F,D,P and ^{2}F,D,P).

configurations of the same parity: 4d^2, 4d5s and 5s^2, resulting in eight parent terms for the 4d^{2}nl, 4d5snl and 5s^{2}nl configurations in Zr II. The lowest parent term, 4d^2 ^{3}F, is the ionization limit for Zr II. The *LS* terms involved in this work belong to 4d^{2}5p and 4d5s5p of odd parity and 4d^3, 4d^{2}5s and 4d5s^2 of even parity, and they are plotted in the term diagram in Fig. 1. As can be seen in the figure the distance between 5p and 5s is about 20 000–40 000 cm^{-1} for all the transitions, and the spectral lines occur consequently in the wavelength interval 2500–5000 Å.

3. Experimental oscillator strengths

The oscillator strength f is related to the transition probability A_{ik}:

$$f = 1.499 \times 10^{-16} \frac{g_i \lambda^2}{g_k} A_{ik}, \tag{1}$$

where g_i and g_k are the statistical weights for the upper and lower level, λ is the wavelength in Å of the transition, and A_{ik} is the transition probability in s^{-1}.

The transition probability is derived from the BF and the lifetime (τ_i) of the upper level,

$$A_{ik} = \frac{BF_{ik}}{\tau_i}. \tag{2}$$

Absolute A_{ik}-values (and thus f-values) are obtained from experimental data on BFs and lifetimes.

3.1. Branching fractions (BFs)

The BF of an emission line is related to the transition probability or the intensity for the line:

$$BF_{ik} = \frac{A_{ik}}{\sum_j A_{ij}} = \frac{I_{ik}}{\sum_j I_{ij}}, \tag{3}$$

where A_{ik} is the transition probability of the line from the upper level i to the lower level k, and I_{ik} is the intensity of the line. The sums are over all possible transitions originating from the same upper level i.

The intensities, from which the BFs are derived, were measured with the Chelsea Instrument FT500 UV FTS in Lund. The light source was a hollow cathode (HC) discharge lamp with a cathode of pure zirconium. Spectra were recorded at a current of 0.4 A, a voltage of 500 V and a pressure of 0.6 torr of the argon carrier gas. The recordings were made in two intervals, 20 500–41 000 cm^{-1} and 17 400–34 800 cm^{-1}, because of the use of two different detectors. An extract of the spectrum is shown in Fig. 2. The measurements in the spectra were made with the program Xgremlin (Nave et al. 1997) (based on the Decomp code by Brault & Adams 1989), where a Voigt profile was fitted to the line. The measured equivalent width of the fitted emission line was used as a measure of the intensity.

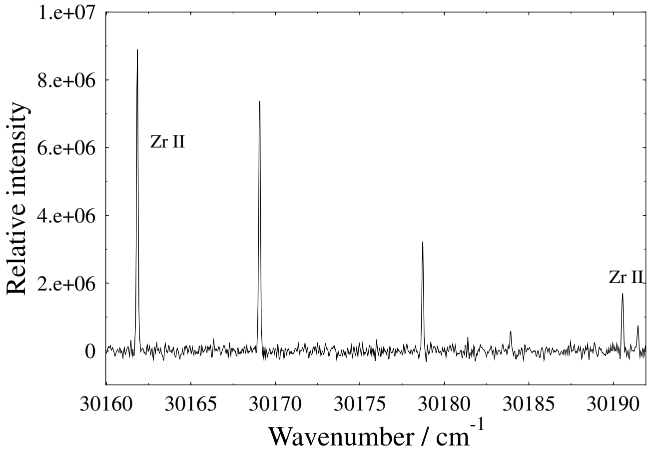

Fig. 2. The marked lines are Zr II lines from the same upper level z^{2}P$_{3/2}$, with BFs 0.097 and 0.018. The other two lines are Zr II (at 30 169 cm^{-1}) and Ar II (at 30 178 cm^{-1}).

The intensity calibration of the spectra was made with known branching ratios (BRs) for argon lines (Whaling et al. 1993; Hashiguchi & Hasikuni 1985), and the instrument response function was constructed by comparing with BRs derived from the intensities measured in our spectra. Argon is suitable for calibration since it covers a wide wavelength interval, and there are levels with many branches distributed over the relevant frequency interval.

Strong lines to low energy levels can be affected by self-absorption, i.e. the measured intensity becomes too small since the population of the lower level is high and photons can be reabsorbed in the light source. The effect of self absorption is checked by measuring the BR of one optically thick and one optically thin line for different level populations. This was performed by measuring BRs at different currents for all potentially optically thick lines. Interferograms with currents from 0.15 to 0.50 A in steps of 0.05 A (two for each current) were recorded with the HC lamp burning at the same gas pressure. A plot of the BR against the current shows either a horizontal straight line or a straight line with a slope. The horizontal line indicates that there is no self-absorption, but a tilted line is an indication that at least one of the two spectral lines defining the BR is influenced by self-absorption. The graph is extrapolated to zero current which represents the optically thin case. Thus, the BR adopted is the value obtained for zero current.

Since the lines were measured in two different spectral regions the intensity calibration had to be set on the same scale. This was done by measuring the intensities for as many lines as possible in the overlapping region and deriving a normalization factor, *viz.* the mean ratio between the two intensities measured for each line.

The BF is defined as the transition probability of a line divided by the sum of the transition probabilities of all lines from the same upper level (Eq. (3)). But, if all lines cannot be measured the intensity sum will not be correct. Lines can for example be missing because they are too weak to be measured

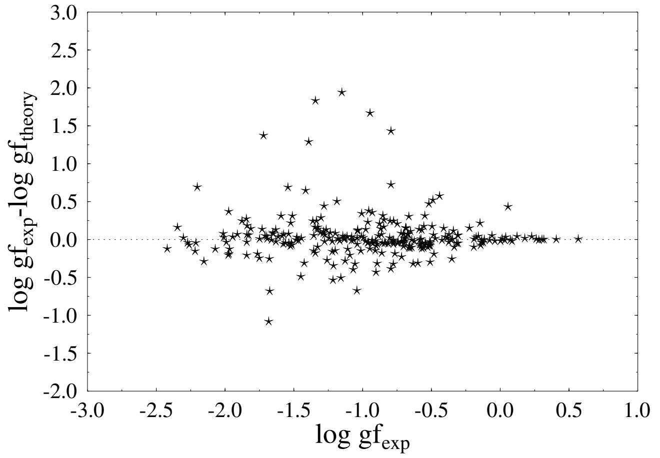

Fig. 3. Comparison between experimental and theoretical log gf-values from this work.

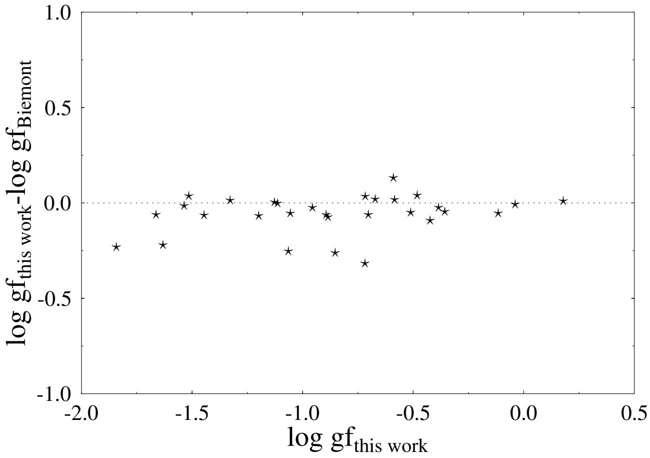

Fig. 4. Comparison between log gf-values from this work and the work of Biémont et al. (1981).

accurately or are located outside the recorded wavelength interval. Theoretical calculations of BFs using the Cowan (1981) code were used to estimate the intensity of the missing spectral lines. The calculations included the even configurations 4d^{2}5s, 4d^3, 4d5s^2, 4d^{2}6s, 4d^{2}5d, 4d5s6s, 4d5p^2, 4d5s5d, 4d^{2}7s, 4d^{2}6d, 4d^{2}5g, 4d^{2}7d, 4d5s6d, 5s^{2}6s, 5s^{2}5d, 5s^{2}6d and 4d5d^2, and the odd configurations 4d^{2}5p, 4d5s5p, 5s^{2}5p, 4d^{2}6p, 4d^{2}4f, 4d^{2}7p, 4d5s4f, 4d5s6p, 4d5s7p, 5s^{2}6p, 4d5p5d, 5s^{2}4f and 5p^3. A parametric fit of the calculated energy levels to observed energies for some of the configurations was made to obtain the final wavefunctions. The calculations are part of an ongoing project on the term analysis of Zr II, including a large number of new energy levels.

The experimental log gf values are compared with the theoretical ones in Fig. 3, and predicted BFs for missing lines (the residuals) are reported in Table 2. The theoretical BFs are scaled with the experimental lifetimes and are in most cases in agreement with the experimental ones. Experimental intensities indicate however that some levels have a strong mixing, which is not fully reproduced by the calculations. This is especially true for the term y^{4}D, but since the residuals are small (1–4%), even a more sophisticated calculation would not change the residuals more than a few percent.

3.2. Oscillator strengths

From Eqs. (1) and (2) the oscillator strength can be derived using the BF and the lifetime.

The uncertainty in the oscillator strength and transition probability is almost the same, since f is proportional to $\lambda^2 A$, and the uncertainties in wavelengths are much smaller than those in A-values. The uncertainty in the transition probability, $u(A_{ik})$ is dependent on the uncertainties in the BFs, i.e. the intensities, and in the lifetimes, and they are assumed to be uncorrelated. The relative uncertainty $u_{\rm r}(A_{ik})$ of the transition probability A_{ik} is given by (Sikström et al. 2002):

$$u_{\rm r}^2(A_{ik}) = \left(\frac{u(A_{ik})}{A_{ik}}\right)^2 = (1 - BF_{ik})^2\left(\frac{u(I_{ik})}{I_{ik}}\right)^2 + \sum_{j\neq k} BF_{ij}^2\left(\frac{u(I_{ij})}{I_{ij}}\right)^2 + q^2(BF_{\rm res})^2 + \left(\frac{u(\tau_i)}{\tau_i}\right)^2, \quad (4)$$

where $\left(\frac{u(I_{ij})}{I_{ij}}\right)$ is the relative uncertainty in the intensity and $\left(\frac{u(\tau_i)}{\tau_i}\right)$ is the relative uncertainty in the measured lifetime. The sum is taken over all the lines originating from the same upper level as the line in question. $BF_{\rm res}$ is the BF for the missing lines, the residual, and the constant q in front is a measure of the uncertainty in the residual. Sources of uncertainty are the lifetime measurements, intensity measurements, calibration, self-absorption and connection of measurements in different spectra. These are calculated and the combined relative uncertainties in the oscillator strengths are given in the tables among the other results.

In this work the transitions from 34 energy levels of Zr II have been investigated, and oscillator strengths for 263 Zr II lines have been determined by combining experimental BFs and radiative lifetimes. The lifetimes used to derive oscillator strengths from the BF-values were taken from different papers (Langhans et al. 1995; Biémont et al. 1981; Sikström et al. 1999). The experimental and theoretical BFs and the f-values are given in Table 2, where the lines are sorted by upper level. Ritz wavelengths and level designations are taken from an ongoing term analysis of Zr II, based on FTS spectra.

A finding list with the log gf-values for in total 263 Zr II lines are given in Table 3.

The uncertainties of the oscillator strengths are in most groups around 10%, but in some cases higher. The high values may be due to low signal-to-noise ratio or high uncertainty in the calibration for lines above 37 000 cm^{-1}. Recording with a detector sensitive in that region was made but the different recordings could not be connected.

Only one line was found to be blended with argon and therefore much stronger than expected. Recordings with neon instead of argon showed that the Zr II line was too weak to be measured and therefore included in the residual.

Comparisons with previous determinations of log gf-values are shown in Figs. 4–6 (note the different scales). Our new values agree with those of Biémont et al. (1981) but are in general a bit higher. The scatter is larger when comparing to Bogdanovich et al. (1995), which is to be expected since that work only included theoretical calculations. Compared to Malcheva et al. (2006) most of the lines are in good agreement. In Fig. 7 our experimental and theoretical oscillator strengths are compared for the set of lines shown in Fig. 6. By comparing Figs. 7 with 6 it can be seen that the two different theoretical approaches give almost the same results. The lines deviating strongly in both

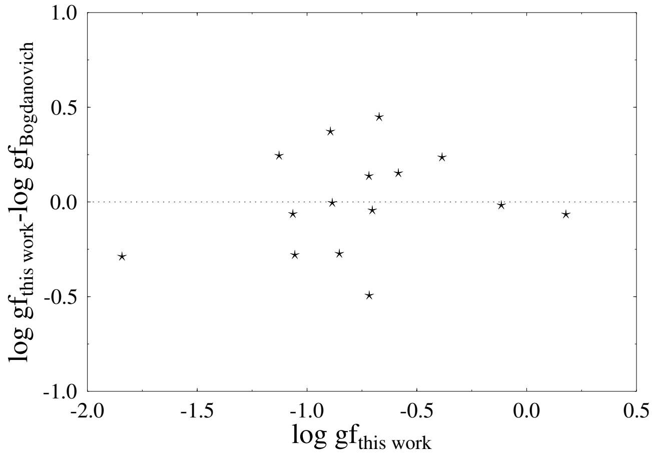

Fig. 5. Comparison between log gf-values from this work and the work of Bogdanovich et al. (1995).

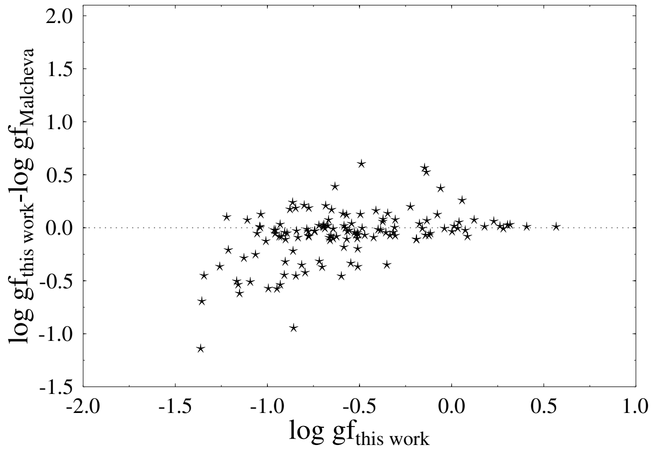

Fig. 6. Comparison between log gf-values from this work and the work of Malcheva et al. (2006).

diagrams are those we had problems with reproducing in the theoretical calculations, as discussed in Sect. 3.1.

4. Solar abundance analysis

The most obvious application of the presented transition probabilities for Zr II lines is in stellar elemental abundance analyses. As an example of the improved accuracy that can now be achieved, we have revisited the issue of the solar Zr abundance, which has previously been determined by Biémont et al. (1981); Gratton & Sneden (1994) and Bogdanovich et al. (1995). Besides having more accurate atomic line data, we also improve on these studies by employing a time-dependent, 3D, hydrodynamical model of the solar photosphere (Asplund et al. 2000a). This 3D model has in the past few years been applied to new determinations of the solar chemical compositions of all elements up to Ca as well as Fe in a series of articles (Asplund et al. 2000b; Asplund 2000; Asplund et al. 2004; Asplund 2004; Asplund et al. 2005a,b; Allende Prieto et al. 2001, 2002; Scott et al. 2006). For comparison purposes, we have also carried out an analysis using two well-used 1D hydrostatic models: the semi-empirical Holweger & Müller (1974) and the theoretical MARCS (Gustafsson et al. 1975; Asplund et al. 1997) solar model atmospheres.

We have critically evaluated all the solar Zr II lines for which oscillator strengths have been determined in this work, in both the Liège Jungfraujoch (Delbouille et al. 1973) and Brault & Neckel (1987) disk-center solar atlases. We have rejected all lines which are significantly perturbed by blending with atomic or molecular lines or are too weak for a reliable abundance to be determined. We have also rejected those lines where the placement of the continuum level is uncertain. This is one of the largest uncertainties for lines around 3000–4000 Å. In the end, we retained only seven lines for which the relevant line data are given in Table 1. Our sample is still sufficiently large not to be affected by possible spurious effects on individual lines, in particular since the derived abundances agree almost perfectly in all cases, as described below.

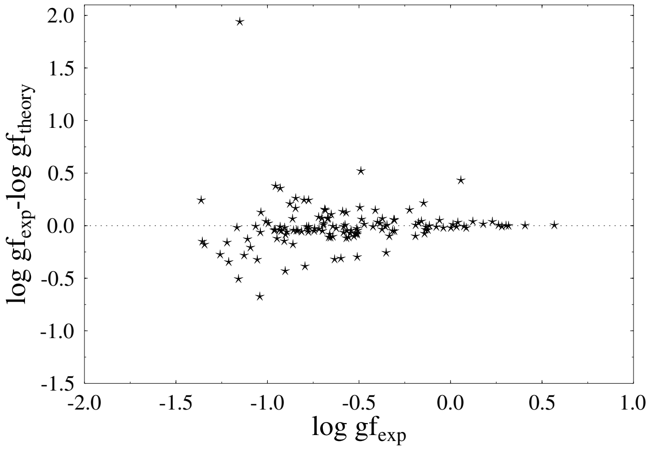

Fig. 7. Comparison between theoretical and experimental log gf-values from this work for the same lines as reported by Malcheva et al. (2006), i.e. the same set of lines as shown in Fig. 6.

Table 1. Solar abundance of Zr II.

λ (Å)	χ_{exc} (eV)	log gf	W_λ (mÅ)	log ε_{Zr} 3D	MARCS	HM
4024.435	0.999	−1.13	12.0	2.56	2.55	2.62
4050.320	0.713	−1.06	22.0	2.57	2.56	2.63
4208.980	0.713	−0.51	42.6	2.54	2.51	2.59
4258.041	0.559	−1.20	23.4	2.57	2.56	2.63
4442.992	1.486	−0.42	20.4	2.58	2.55	2.62
4496.962	0.713	−0.89	31.5	2.60	2.57	2.65
5112.270	1.665	−0.85	7.8	2.61	2.59	2.65

The individual Zr abundances were estimated using profile fitting for the 3D hydrodynamical model atmosphere under the assumption of local thermodynamic equilibrium (LTE) for the spectral line formation. As shown in Asplund et al. (2000a), in 3D there is no need to invoke micro- and macroturbulence in order to achieve the correct theoretical line broadening due to the presence of Doppler shifts from convective motions and temperature inhomogeneities. The equivalent widths of the best-fitting 3D line profiles are given in Table 1 together with the determined Zr abundances. These line strengths have been used to estimate the 1D abundances using the MARCS and Holweger & Müller models, which are also given in Table 1.

The mean 3D LTE-based solar Zr abundance is $\log \varepsilon_{\text{Zr}} = 2.58 \pm 0.02$ where the error is the standard deviation of the individual line abundances. There are no significant trends in abundance with wavelength, excitation potential or line strength. The corresponding results for the MARCS and Holweger & Müller models are $\log \varepsilon_{\text{Zr}} = 2.56 \pm 0.02$ and $\log \varepsilon_{\text{Zr}} = 2.63 \pm 0.02$; as expected for a majority species like Zr II the 3D abundance corrections are relatively minor in the case of the Sun (Asplund 2005).

The derived solar Zr abundance is apparently not very sensitive to the exact choice of model atmosphere with a difference of 0.07 dex between the theoretical MARCS and the semi-empirical Holweger & Müller 1D model atmospheres. Of the three models investigated here, we believe the 3D model is the most realistic due to its proper treatment of convection and accounting for atmospheric inhomogeneities. This 3D hydrodynamic solar model has previously been shown to produce essentially perfect agreement with observed line shapes, shifts and asymmetries (Asplund et al. 2000a) which is not possible with any 1D model. The agreement between different atomic and molecular abundance indicators for C and O is also vastly improved compared with for example the Holweger & Müller model (Asplund et al. 2004, 2005b). We do note, however, that the significantly lower solar C, N and O abundances resulting from a 3D analysis (Asplund et al. 2005a) cause severe problems for solar interior models compared with helioseismology (e.g. Bahcall et al. 2005), which deserves further work to understand.

Compared with previous solar Zr abundance analyses, the line-to-line scatter in our study has decreased dramatically: Biémont et al. (1981) and Gratton & Sneden (1994) for example both obtain a standard deviation of 0.14 dex due to their lower quality transition probabilities and inclusion of less reliable lines; when only considering the six lines in common with our work their standard deviations decrease to 0.11 dex or 0.07 dex when furthermore also removing the 5112.2 Å line. The small difference with the mean abundance of Biémont et al. (1981) is fortuitous as the differences in gf-values (≈ -0.07 dex) are compensated by their equivalent widths typically being larger than those given in Table 1 and their use of the Holweger & Müller (1974) model rather than our 3D hydrodynamical model atmosphere.

5. Conclusions

Oscillator strengths for Zr II have been derived by combining new experimental branching fractions with previously measured radiative lifetimes. 263 spectral lines in the region 2500–5400 Å combine 34 odd parity levels with 29 low metastable levels between 0 and 2.4 eV. All the log gf-values can be found in Table 3.

Based on the new data for Zr II we recommend a solar photospheric Zr abundance of $\log \varepsilon_{\rm Zr} = 2.58 \pm 0.02$. This is in excellent agreement with the meteoritic value of $\log \varepsilon_{\rm Zr} = 2.57 \pm 0.02$ (Asplund et al. 2005a).

References

Allende Prieto, C., Lambert, D. L., & Asplund, M. 2001, ApJ, 556, L63
Allende Prieto, C., Lambert, D. L., & Asplund, M. 2002, ApJ, 573, L137
Asplund, M. 2000, A&A, 359, 755
Asplund, M. 2004, A&A, 417, 769
Asplund, M. 2005, ARA&A, 43, 481
Asplund, M., Gustafsson, B., Kiselman, D., & Eriksson, K. 1997, A&A, 318, 521
Asplund, M., Nordlund, Å., Trampedach, R., Allende Prieto, C., & Stein, R. F. 2000a, A&A, 359, 729
Asplund, M., Nordlund, Å., Trampedach, R., & Stein, R. F. 2000b, A&A, 359, 743
Asplund, M., Grevesse, N., Sauval, A. J., Allende Prieto, C., & Kiselman, D. 2004, A&A, 417, 751
Asplund, M., Grevesse, N., & Sauval, A. J. 2005a, in Cosmic Abundances as Records of Stellar Evolution and Nucleosynthesis, ASP Conf. Ser., 336, 25
Asplund, M., Grevesse, N., Sauval, A. J., Allende Prieto, C., & Blomme, R. 2005b, A&A, 431, 693
Bahcall, J. N., Basu, S., Pinsonneault, M., & Serenelli, A. M. 2005, ApJ, 618, 1049
Biémont, E., Grevesse, N., Hannaford, P., & Lowe, R. M. 1981, ApJ, 248, 867
Bogdanovich, P., Tautvaisiene, G., Rudzikas, Z., & Momkauskaite, A. 1995, in Astrophysical Applications of Powerful New Databases, ASP Conf. Ser., 78, 395
Brault, J., & Neckel, H. 1987, Spectral atlas of solar absolute disk-averaged and disk-center intensity from 3290 to 12 510 Å (available at `ftp.hs.uni-hamburg.de/pub/outgoing/FTS-atlas`)
Brault, J. W., & Adams, M. C. 1989, Opt. Soc. Am. Techn. Digest Series, 6, 110
Busso, M., Gallino, R., & Wasserburg, G. J. 1999, ARA&A, 37, 239
Corliss, C. H., & Bozman, W. R. 1962, Experimental transition probabilities for spectral lines of seventy elements; derived from the NBS Tables of spectral-line intensities (NBS Monograph, Washington: US Department of Commerce, National Bureau of Standards)
Cowan, R. D. 1981, The theory of atomic structure and spectra, Los Alamos Series in Basic and Applied Sciences (Berkeley: University of California Press)
Delbouille, L., Roland, G., & Neven, L. 1973, Atlas photometrique DU spectre solaire de λ 3000 a λ 10000 (Liège: Université de Liège, Institut d'Astrophysique)
Gratton, R. G., & Sneden, C. 1994, A&A, 287, 927
Gustafsson, B., Bell, R. A., Eriksson, K., & Nordlund, A. 1975, A&A, 42, 407
Hashiguchi, S., & Hasikuni, M. 1985, JPSJ, 54, 1290
Holweger, H., & Müller, E. A. 1974, Sol. Phys., 39, 19
Langhans, G., Schade, W., & Helbig, V. 1995, Z. Physik D, 34, 151
Lodders, K. 2003, ApJ, 591, 1220
Malcheva, G., Blagoev, K., Mayo, R., et al. 2006, MNRAS, 367, 754
Nave, G., Sansonetti, C. J., & Griesmann U. 1997, in OSA Technical Digest Ser. Vol 3, Fourier Transform Spectroscopy, Optical Society of America, Washington DC, 38
Scott, P. C., Asplund, M., Grevesse, N., & Sauval, A. J. 2006, A&A, in press
Sikström, C. M., Lundberg, H., Wahlgren, G. M., et al. 1999, A&A, 343, 297
Sikström, C. M., Nilsson, H., Litzén, U., Blom, A., & Lundberg, H. 2002, J. Quant. Spec. Radiat. Transf., 74, 355
Whaling, W., Carle, M. T., & Pitt, M. L. 1993, J. Quant. Spec. Radiat. Transf., 50, 7

Online Material

Table 2. Zr II branching fractions (BFs) and f-values. The lines are sorted by upper level.

Upper Level Lifetime	Lower Level	λ_{air} (Å)	σ (cm^{-1})	*BF* Exp.	 Theory	f Exp.	Unc[d] (%)
$z^4G_{5/2}$	$a^4F_{3/2}$	3572.468	27983.864	0.668	0.686	0.270	5
τ = 7.1(3)ns[a]	$a^4F_{5/2}$	3613.098	27669.191	0.160	0.159	0.044	8
	$a^4F_{7/2}$	3672.664	27220.436	0.004	0.004	0.001	7
	$b^4F_{3/2}$	3934.114	25411.492	0.042	0.044	0.021	6
	$a^2D_{3/2}$	4211.877	23735.699	0.041	0.032	0.023	6
	$a^2D_{5/2}$	4258.041	23478.368	0.028	0.023	0.011	6
	$a^2F_{5/2}$	4496.962	22230.996	0.051	0.046	0.022	6
Residual				0.007			
$z^4G_{7/2}$	$a^4F_{5/2}$	3496.205	28594.257	0.749	0.743	0.305	5
τ = 6.0(3)ns[a]	$a^4F_{7/2}$	3551.951	28145.502	0.174	0.178	0.055	8
	$b^4F_{5/2}$	3843.018	26013.833	0.039	0.043	0.019	7
	$a^2D_{5/2}$	4096.628	24403.434	0.006	0.004	0.003	8
	$a^2F_{5/2}$	4317.309	23156.062	0.010	0.009	0.006	8
	$a^2F_{7/2}$	4454.795	22441.421	0.017	0.016	0.008	7
Residual				0.006			
$z^2F_{5/2}$	$a^4F_{3/2}$	3388.200	29504.900	0.301	0.215	0.097	3
τ = 8.0(2)ns[a]	$a^4F_{5/2}$	3424.822	29190.227	0.035	0.020	0.008	4
	$a^4F_{7/2}$	3478.297	28741.472	0.025	0.026	0.004	4
	$b^4F_{7/2}$	3814.958	26205.168	0.003	0.004	0.001	6
	$a^2D_{3/2}$	3958.220	25256.735	0.274	0.308	0.121	4
	$a^2D_{5/2}$	3998.965	24999.404	0.168	0.203	0.050	4
	$a^2F_{5/2}$	4208.980	23752.032	0.155	0.182	0.051	4
	$a^2P_{3/2}$	4273.513	23393.371	0.016	0.016	0.008	4
	$a^2F_{7/2}$	4339.549	23037.391	0.005	0.005	0.001	5
	$a^2G_{7/2}$	4613.946	21667.354	0.012	0.014	0.004	5
Residual				0.006			
$z^4F_{3/2}$	$a^4F_{3/2}$	3357.261	29777.624	0.206	0.268	0.055	5
τ = 6.3(3)ns[a]	$a^4F_{5/2}$	3393.119	29462.951	0.164	0.185	0.030	6
	$b^4F_{3/2}$	3674.714	27205.252	0.242	0.270	0.078	6
	$b^4F_{5/2}$	3718.830	26882.527	0.013	0.020	0.003	6
	$a^2D_{3/2}$	3915.934	25529.459	0.098	0.067	0.036	6
	$a^2P_{1/2}$	4156.232	24053.474	0.102	0.059	0.084	6
	$a^2F_{5/2}$	4161.200	24024.756	0.156	0.115	0.043	6
	$a^2P_{3/2}$	4224.264	23666.095	0.008	0.004	0.003	6
Residual				0.011			
$z^4G_{9/2}$	$a^4F_{7/2}$	3438.231	29076.393	0.829	0.830	0.319	3
τ = 5.75(20)ns[a]	$a^4F_{9/2}$	3505.666	28517.091	0.129	0.123	0.041	8
	$b^4F_{7/2}$	3766.815	26540.089	0.040	0.044	0.018	7
Residual				0.003			
$z^2D_{3/2}$	$a^4F_{3/2}$	3284.712	30435.303	0.472	0.406	0.106	5
τ = 7.2(3)ns[a]	$a^4F_{5/2}$	3319.029	30120.630	0.057	0.021	0.009	6
	$b^4F_{3/2}$	3587.974	27862.931	0.148	0.085	0.040	6
	$b^4F_{5/2}$	3630.020	27540.206	0.070	0.064	0.013	6
	$a^2D_{3/2}$	3817.585	26187.138	0.061	0.118	0.019	6
	$a^2P_{1/2}$	4045.613	24711.153	0.101	0.153	0.069	6
	$a^2F_{5/2}$	4050.320	24682.435	0.064	0.136	0.015	6
	$b^4P_{3/2}$	4831.327	20692.464	0.010	0.000	0.005	7
Residual				0.016			
$z^2F_{7/2}$	$a^4F_{5/2}$	3305.152	30247.083	0.140	0.110	0.037	5
τ = 8.2(4)ns[a]	$a^4F_{9/2}$	3419.106	29239.026	0.013	0.011	0.002	6
	$b^4F_{7/2}$	3667.062	27262.024	0.004	0.007	0.001	7

Table 2. continued.

Upper Level	Lower	λ_{air}	σ	*BF*		*f*	Unc[d]
Lifetime	Level	(Å)	(cm^{-1})	Exp.	Theory	Exp.	(%)
	b^{4}F$_{9/2}$	3729.722	26804.024	0.014	0.015	0.003	5
	a^{2}D$_{5/2}$	3836.761	26056.260	0.356	0.358	0.128	5
	a^{2}F$_{5/2}$	4029.675	24808.888	0.070	0.076	0.028	5
	a^{2}F$_{7/2}$	4149.198	24094.247	0.363	0.383	0.114	5
	a^{4}P$_{5/2}$	4442.500	22503.528	0.004	0.004	0.002	7
	a^{2}G$_{9/2}$	4461.217	22409.117	0.025	0.025	0.007	5
Residual				0.012			
z^{4}G$_{11/2}$	a^{4}F$_{9/2}$	3391.971	29472.919	0.963	0.958	0.369	7
τ = 5.4(4)ns[c]	b^{4}F$_{9/2}$	3697.457	27037.917	0.037	0.042	0.017	10
Residual				0.000			
z^{2}D$_{5/2}$	a^{4}F$_{3/2}$	3208.313	31160.024	0.010	0.004	0.003	7
τ = 8.4(4)ns[a]	a^{4}F$_{5/2}$	3241.044	30845.351	0.239	0.180	0.045	5
	b^{4}F$_{3/2}$	3497.013	28587.652	0.005	0.001	0.002	8
	b^{4}F$_{5/2}$	3536.943	28264.927	0.029	0.007	0.006	6
	b^{4}F$_{7/2}$	3588.314	27860.292	0.054	0.052	0.009	5
	a^{2}D$_{3/2}$	3714.777	26911.859	0.075	0.032	0.028	5
	a^{2}D$_{5/2}$	3750.642	26654.528	0.024	0.073	0.006	6
	a^{2}F$_{5/2}$	3934.785	25407.156	0.075	0.079	0.021	5
	a^{2}P$_{3/2}$	3991.127	25048.495	0.290	0.327	0.124	5
	a^{2}F$_{7/2}$	4048.666	24692.515	0.169	0.214	0.037	5
	a^{2}G$_{7/2}$	4286.503	23322.478	0.012	0.011	0.003	6
Residual				0.019			
z^{4}F$_{7/2}$	a^{4}F$_{5/2}$	3231.692	30934.615	0.127	0.123	0.056	7
τ = 4.7(3)ns[c]	a^{4}F$_{7/2}$	3279.264	30485.860	0.483	0.444	0.166	7
	a^{4}F$_{9/2}$	3340.553	29926.558	0.095	0.107	0.027	7
	b^{4}F$_{5/2}$	3525.807	28354.191	0.035	0.038	0.018	7
	b^{4}F$_{7/2}$	3576.853	27949.556	0.230	0.254	0.094	7
	b^{4}F$_{9/2}$	3636.444	27491.556	0.017	0.016	0.006	7
	a^{2}D$_{5/2}$	3738.123	26743.792	0.004	0.007	0.002	8
	a^{2}F$_{7/2}$	4034.083	24781.779	0.007	0.009	0.004	8
Residual				0.002			
z^{4}F$_{9/2}$	a^{4}F$_{7/2}$	3214.189	31103.065	0.117	0.109	0.050	7
τ = 4.55(20)ns[a]	a^{4}F$_{9/2}$	3273.047	30543.763	0.570	0.572	0.201	5
	b^{4}F$_{7/2}$	3499.571	28566.761	0.021	0.022	0.011	7
	b^{4}F$_{9/2}$	3556.594	28108.761	0.284	0.290	0.119	6
	a^{2}F$_{7/2}$	3936.051	25398.984	0.005	0.006	0.003	7
Residual				0.002			
z^{4}D$_{1/2}$	a^{4}F$_{3/2}$	3125.919	31981.317	0.484	0.545	0.050	5
τ = 7.1(3)ns[b]	b^{4}F$_{3/2}$	3399.350	29408.945	0.390	0.325	0.048	6
	a^{2}P$_{1/2}$	3807.403	26257.167	0.008	0.008	0.002	11
	a^{4}P$_{1/2}$	4085.719	24468.588	0.020	0.022	0.007	49
	b^{4}P$_{1/2}$	4457.413	22428.244	0.072	0.076	0.030	6
	b^{4}P$_{3/2}$	4495.449	22238.478	0.017	0.015	0.004	7
Residual				0.008			
z^{4}D$_{3/2}$	a^{4}F$_{3/2}$	3099.228	32256.741	0.130	0.145	0.027	7
τ = 6.9(4)ns[c]	a^{4}F$_{5/2}$	3129.760	31942.068	0.336	0.376	0.048	6
	b^{4}F$_{3/2}$	3367.809	29684.369	0.050	0.041	0.012	7
	b^{4}F$_{5/2}$	3404.827	29361.644	0.324	0.284	0.054	7
	a^{2}D$_{3/2}$	3569.316	28008.576	0.005	0.005	0.001	10
	a^{2}P$_{1/2}$	3767.879	26532.591	0.014	0.014	0.009	7
	a^{2}F$_{5/2}$	3771.962	26503.873	0.005	0.007	0.001	9

Table 2. continued.

Upper Level	Lower	$\lambda_{\rm air}$	σ	BF		f	Unc^d
Lifetime	Level	(Å)	(cm^{-1})	Exp.	Theory	Exp.	(%)
	a^{4}P$_{1/2}$	4040.240	24744.012	0.016	0.013	0.011	7
	a^{4}P$_{3/2}$	4077.046	24520.637	0.014	0.014	0.005	7
	b^{4}P$_{1/2}$	4403.338	22703.668	0.039	0.039	0.033	7
	b^{4}P$_{3/2}$	4440.453	22513.902	0.053	0.051	0.023	7
	b^{4}P$_{5/2}$	4485.444	22288.081	0.006	0.005	0.002	9
Residual				0.007			
z^{4}D$_{5/2}$	a^{4}F$_{3/2}$	3065.207	32614.743	0.009	0.012	0.003	8
τ = 7.0(3)ns^b	a^{4}F$_{5/2}$	3095.070	32300.070	0.117	0.131	0.024	5
	a^{4}F$_{7/2}$	3138.678	31851.315	0.334	0.364	0.053	5
	b^{4}F$_{5/2}$	3363.811	29719.646	0.040	0.033	0.010	5
	b^{4}F$_{7/2}$	3410.243	29315.011	0.328	0.289	0.061	5
	a^{2}F$_{5/2}$	3721.690	26861.875	0.002	0.003	0.001	10
	a^{2}P$_{3/2}$	3772.056	26503.214	0.013	0.014	0.006	6
	a^{2}F$_{7/2}$	3823.411	26147.234	0.005	0.006	0.001	7
	a^{4}P$_{3/2}$	4018.377	24878.639	0.026	0.022	0.013	5
	a^{4}P$_{5/2}$	4071.089	24556.515	0.010	0.010	0.004	6
	b^{4}P$_{3/2}$	4370.948	22871.904	0.068	0.070	0.042	5
	b^{4}P$_{5/2}$	4414.535	22646.083	0.033	0.031	0.014	5
Residual				0.015			
z^{4}D$_{7/2}$	a^{4}F$_{7/2}$	3110.874	32135.985	0.074	0.090	0.016	5
τ = 6.8(2)ns^b	a^{4}F$_{9/2}$	3165.977	31576.683	0.415	0.429	0.073	5
	b^{4}F$_{7/2}$	3377.445	29599.681	0.022	0.020	0.006	5
	b^{4}F$_{9/2}$	3430.527	29141.681	0.334	0.305	0.069	5
	a^{2}D$_{5/2}$	3520.874	28393.917	0.024	0.020	0.009	5
	a^{2}F$_{7/2}$	3782.232	26431.904	0.006	0.005	0.002	6
	a^{4}P$_{5/2}$	4024.435	24841.185	0.026	0.026	0.012	5
	b^{4}P$_{5/2}$	4359.730	22930.753	0.092	0.098	0.051	5
Residual				0.008			
y^{2}D$_{3/2}$	a^{4}F$_{3/2}$	3030.919	32983.686	0.144	0.108	0.023	4
τ = 8.6(3)ns^a	a^{4}F$_{5/2}$	3060.115	32669.013	0.046	0.056	0.005	5
	b^{4}F$_{3/2}$	3287.303	30411.314	0.026	0.023	0.005	5
	a^{2}D$_{3/2}$	3479.017	28735.521	0.252	0.218	0.053	4
	a^{2}D$_{5/2}$	3510.455	28478.190	0.106	0.124	0.015	5
	a^{2}F$_{5/2}$	3671.264	27230.818	0.277	0.284	0.043	5
	b^{2}D$_{3/2}$	5112.270	19555.330	0.077	0.037	0.035	5
	c^{2}D$_{3/2}$	5350.350	18685.175	0.035	0.112	0.017	5
Residual				0.037			
z^{2}G$_{7/2}$	a^{2}D$_{5/2}$	3334.616	29979.842	0.073	0.070	0.034	7
τ = 4.8(3)ns^a	a^{2}F$_{5/2}$	3479.387	28732.470	0.499	0.484	0.251	6
	a^{2}F$_{7/2}$	3568.137	28017.829	0.015	0.010	0.006	7
	a^{2}G$_{7/2}$	3751.590	26647.792	0.286	0.301	0.126	7
	a^{2}G$_{9/2}$	3796.482	26332.699	0.035	0.041	0.013	7
	a^{2}H$_{9/2}$	4442.992	22501.039	0.076	0.079	0.038	7
Residual				0.016			
z^{2}P$_{3/2}$	a^{2}D$_{3/2}$	3156.994	31666.530	0.077	0.079	0.029	10
τ = 3.9(3)ns^a	a^{2}D$_{5/2}$	3182.860	31409.199	0.662	0.650	0.172	8
	a^{2}P$_{1/2}$	3311.342	30190.545	0.018	0.020	0.015	10
	a^{2}F$_{5/2}$	3314.495	30161.827	0.097	0.100	0.027	10
	a^{2}P$_{3/2}$	3354.384	29803.166	0.069	0.077	0.030	10
	a^{4}P$_{5/2}$	3588.806	27856.467	0.008	0.006	0.003	11
	b^{4}P$_{3/2}$	3819.814	26171.856	0.002	0.001	0.001	15
	b^{4}P$_{5/2}$	3853.061	25946.035	0.005	0.005	0.002	11

Table 2. continued.

Upper Level	Lower	λ_{air}	σ	*BF*		*f*	Unc[d]
Lifetime	Level	(Å)	(cm^{-1})	Exp.	Theory	Exp.	(%)
Residual				0.062			
$y^4D_{1/2}$	$a^4F_{3/2}$	2758.806	36236.851	0.415	0.279	0.070	7
τ = 3.4(2)ns[b]	$b^4F_{3/2}$	2969.623	33664.479	0.259	0.276	0.050	10
	$a^2D_{3/2}$	3125.199	31988.686	0.050	0.029	0.011	11
	$a^2P_{3/2}$	3318.512	30125.322	0.073	0.001	0.018	11
	$a^4P_{1/2}$	3480.398	28724.122	0.156	0.332	0.084	11
	$a^4P_{3/2}$	3507.677	28500.747	0.035	0.071	0.009	11
Residual				0.011			
$y^4F_{3/2}$	$a^4F_{3/2}$	2742.554	36451.585	0.760	0.834	0.182	4
τ = 4.7(2)ns[a]	$b^4F_{5/2}$	2979.180	33556.488	0.126	0.070	0.024	17
	$a^2F_{5/2}$	3256.526	30698.717	0.007	0.007	0.002	19
	$a^4P_{1/2}$	3454.572	28938.856	0.031	0.023	0.024	17
	$a^4P_{3/2}$	3481.445	28715.481	0.029	0.020	0.011	17
Residual				0.047			
$y^4D_{3/2}$	$a^4F_{5/2}$	2752.202	36323.806	0.502	0.308	0.119	6
τ = 3.2(2)ns[a]	$b^4F_{3/2}$	2934.611	34066.107	0.065	0.069	0.026	12
	$b^4F_{5/2}$	2962.679	33743.382	0.162	0.201	0.044	12
	$a^4P_{1/2}$	3432.404	29125.750	0.087	0.148	0.096	12
	$a^4P_{3/2}$	3458.932	28902.375	0.147	0.230	0.082	12
	$a^4P_{5/2}$	3497.919	28580.251	0.009	0.017	0.003	13
Residual				0.028			
$y^4F_{5/2}$	$a^4F_{3/2}$	2711.508	36868.920	0.105	0.100	0.039	14
τ = 4.4(2)ns[a]	$a^4F_{5/2}$	2734.851	36554.247	0.570	0.509	0.145	6
	$b^4F_{7/2}$	2978.053	33569.188	0.109	0.093	0.025	14
	$a^2D_{3/2}$	3064.642	32620.755	0.024	0.036	0.011	14
	$a^2F_{5/2}$	3212.847	31116.052	0.038	0.062	0.013	14
	$a^2F_{7/2}$	3288.374	30401.411	0.005	0.007	0.001	16
	$a^4P_{3/2}$	3431.571	29132.816	0.047	0.062	0.028	14
	$a^2G_{7/2}$	3443.562	29031.374	0.051	0.072	0.015	14
	$a^4P_{5/2}$	3469.940	28810.692	0.018	0.025	0.007	14
	$b^2D_{3/2}$	4264.908	23440.564	0.006	0.005	0.006	14
Residual				0.028			
$y^4D_{5/2}$	$a^4F_{5/2}$	2712.419	36856.529	0.063	0.060	0.017	9
τ = 4.1(2)ns[a]	$a^4F_{7/2}$	2745.854	36407.774	0.299	0.266	0.062	6
	$b^4F_{3/2}$	2889.424	34598.830	0.011	0.010	0.005	13
	$b^4F_{5/2}$	2916.630	34276.105	0.042	0.056	0.013	9
	$b^4F_{7/2}$	2951.475	33871.470	0.090	0.139	0.021	8
	$a^2D_{3/2}$	3036.503	32923.037	0.054	0.032	0.027	9
	$a^2D_{5/2}$	3060.425	32665.706	0.078	0.003	0.027	8
	$a^2F_{5/2}$	3181.935	31418.334	0.080	0.050	0.030	8
	$a^4P_{3/2}$	3396.330	29435.098	0.092	0.193	0.058	8
	$a^2G_{7/2}$	3408.076	29333.656	0.085	0.043	0.027	8
	$a^4P_{5/2}$	3433.910	29112.974	0.049	0.103	0.021	8
	$b^2D_{3/2}$	4210.609	23742.846	0.017	0.005	0.016	9
Residual				0.041			
$y^2F_{5/2}$	$a^4F_{5/2}$	2699.604	37031.483	0.036	0.038	0.011	10
τ = 3.5(2)ns[a]	$a^4F_{7/2}$	2732.721	36582.728	0.169	0.051	0.040	7
	$b^4F_{5/2}$	2901.818	34451.059	0.014	0.007	0.005	10
	$b^4F_{7/2}$	2936.307	34046.424	0.060	0.037	0.017	8
	$a^2D_{3/2}$	3020.452	33097.991	0.119	0.154	0.069	7
	$a^2F_{5/2}$	3164.313	31593.288	0.180	0.228	0.077	7

Table 2. continued.

Upper Level	Lower	λ_{air}	σ	*BF*		*f*	Unc[d]
Lifetime	Level	(Å)	(cm^{-1})	Exp.	Theory	Exp.	(%)
	$a^4P_{3/2}$	3376.262	29610.052	0.047	0.040	0.034	7
	$a^2G_{7/2}$	3387.869	29508.610	0.245	0.292	0.090	7
	$a^4P_{5/2}$	3413.397	29287.928	0.024	0.022	0.012	8
	$b^2D_{3/2}$	4179.808	23917.800	0.046	0.033	0.052	8
	$b^2G_{7/2}$	4293.125	23286.505	0.020	0.029	0.012	8
	$b^2D_{5/2}$	4312.225	23183.362	0.005	0.003	0.004	10
	$c^2D_{3/2}$	4337.619	23047.644	0.013	0.043	0.015	8
Residual				0.022			
$y^4F_{7/2}$	$a^4F_{5/2}$	2693.524	37115.071	0.052	0.039	0.018	9
$\tau = 4.3(2)$ns[a]	$a^4F_{7/2}$	2726.491	36666.316	0.288	0.205	0.075	7
	$a^4F_{9/2}$	2768.727	36107.014	0.055	0.024	0.012	9
	$b^4F_{9/2}$	2968.959	33672.012	0.115	0.136	0.028	8
	$a^2D_{5/2}$	3036.391	32924.248	0.101	0.118	0.043	8
	$a^2F_{5/2}$	3155.963	31676.876	0.004	0.006	0.002	12
	$a^2F_{7/2}$	3228.809	30962.235	0.106	0.129	0.039	8
	$a^2G_{7/2}$	3378.299	29592.198	0.015	0.019	0.006	9
	$a^4P_{5/2}$	3403.682	29371.516	0.078	0.160	0.042	8
	$a^2G_{9/2}$	3414.659	29277.105	0.140	0.108	0.046	8
	$b^2D_{5/2}$	4296.733	23266.950	0.019	0.009	0.016	8
	$b^2G_{9/2}$	4301.801	23239.541	0.012	0.017	0.006	9
	$c^2D_{5/2}$	4404.730	22696.490	0.004	0.019	0.004	11
Residual				0.010			
$z^4S_{3/2}$	$a^2D_{3/2}$	2990.129	33433.623	0.011	0.006	0.004	12
$\tau = 4.2(3)$ns[a]	$a^2D_{5/2}$	3013.323	33176.292	0.040	0.032	0.009	8
	$a^2P_{3/2}$	3166.622	31570.259	0.010	0.007	0.004	10
	$a^4P_{1/2}$	3313.700	30169.059	0.086	0.063	0.068	7
	$a^4P_{3/2}$	3338.419	29945.684	0.133	0.114	0.053	7
	$a^4P_{5/2}$	3374.722	29623.560	0.397	0.394	0.107	7
	$b^4P_{1/2}$	3554.071	28128.714	0.085	0.097	0.077	7
	$b^4P_{3/2}$	3578.211	27938.949	0.120	0.146	0.055	7
	$b^4P_{5/2}$	3607.369	27713.128	0.107	0.132	0.033	7
Residual				0.011			
$y^2F_{7/2}$	$a^4F_{5/2}$	2667.793	37473.029	0.067	0.074	0.023	11
$\tau = 4.1(2)$ns[a]	$a^4F_{7/2}$	2700.130	37024.274	0.392	0.405	0.105	6
	$a^4F_{9/2}$	2741.547	36464.972	0.057	0.154	0.013	11
	$b^4F_{7/2}$	2898.712	34487.970	0.024	0.036	0.008	11
	$a^2D_{5/2}$	3003.733	33282.206	0.107	0.052	0.047	10
	$a^2F_{7/2}$	3191.905	31320.193	0.102	0.035	0.038	10
	$a^2G_{7/2}$	3337.921	29950.156	0.009	0.002	0.004	11
	$a^4P_{5/2}$	3362.699	29729.474	0.027	0.130	0.015	11
	$a^2G_{9/2}$	3373.412	29635.063	0.109	0.029	0.036	10
	$b^2D_{5/2}$	4231.629	23624.908	0.031	0.006	0.027	10
	$c^2D_{5/2}$	4336.338	23054.448	0.003	0.006	0.003	13
Residual				0.072			
$y^4D_{7/2}$	$a^4F_{9/2}$	2722.609	36718.596	0.423	0.157	0.114	7
$\tau = 3.3(2)$ns[a]	$b^4F_{9/2}$	2915.993	34283.594	0.103	0.070	0.032	11
	$a^2D_{5/2}$	2981.015	33535.830	0.050	0.122	0.027	11
	$a^2F_{7/2}$	3166.265	31573.817	0.085	0.169	0.039	11
	$a^2G_{7/2}$	3309.891	30203.780	0.014	0.026	0.007	12
	$a^4P_{5/2}$	3334.253	29983.098	0.111	0.110	0.075	11
	$a^2G_{9/2}$	3344.786	29888.687	0.109	0.199	0.045	11
	$b^2D_{5/2}$	4186.682	23878.532	0.028	0.030	0.030	11
	$b^2G_{9/2}$	4191.493	23851.123	0.013	0.034	0.009	11

Table 2. continued.

Upper Level	Lower	$\lambda_{\rm air}$	σ	*BF*		f	Unc[d]
Lifetime	Level	(Å)	(cm^{-1})	Exp.	Theory	Exp.	(%)
	$c^2D_{5/2}$	4289.152	23308.072	0.003	0.038	0.003	16
	$b^2F_{7/2}$	5372.466	18608.250	0.015		0.019	12
Residual				0.045			
$z^4P_{3/2}$	$a^4F_{5/2}$	2643.396	37818.857	0.066	0.059	0.004	8
τ = 10.6(3)ns[a]	$a^4P_{1/2}$	3264.813	30620.801	0.102	0.227	0.031	4
	$a^4P_{3/2}$	3288.805	30397.426	0.314	0.341	0.048	4
	$b^4P_{1/2}$	3497.893	28580.457	0.042	0.036	0.014	5
	$b^4P_{3/2}$	3521.274	28390.691	0.058	0.003	0.010	5
	$b^4P_{5/2}$	3549.508	28164.870	0.268	0.291	0.032	4
	$c^2D_{5/2}$	4272.251	23400.276	0.110	0.002	0.019	4
Residual				0.041			
$y^4F_{9/2}$	$a^4F_{7/2}$	2639.080	37880.702	0.101	0.086	0.027	21
τ = 4.9(2)ns[b]	$a^4F_{9/2}$	2678.632	37321.400	0.870	0.890	0.191	5
	$b^4F_{9/2}$	2865.605	34886.398	0.022	0.016	0.005	21
Residual				0.008			
$x^4D_{1/2}$	$a^4F_{3/2}$	2567.637	38934.642	0.778	0.733	0.167	4
τ = 2.3(1)ns[b]	$a^4P_{1/2}$	3181.572	31421.913	0.164	0.212	0.108	39
	$a^4P_{3/2}$	3204.352	31198.538	0.020	0.017	0.007	40
Residual				0.038			
$x^4D_{3/2}$	$a^4F_{3/2}$	2550.744	39192.484	0.134	0.137	0.057	32
τ = 2.3(1)ns[b]	$a^4F_{5/2}$	2571.391	38877.811	0.636	0.596	0.183	8
	$a^4P_{1/2}$	3155.676	31679.755	0.104	0.137	0.135	33
	$a^4P_{3/2}$	3178.086	31456.380	0.090	0.096	0.059	33
	$b^4P_{3/2}$	3394.652	29449.645	0.011	0.010	0.008	33
Residual				0.025			
$x^4D_{5/2}$	$a^4F_{5/2}$	2542.112	39325.565	0.090	0.115	0.038	33
τ = 2.3(1)ns[b]	$a^4F_{7/2}$	2571.457	38876.810	0.655	0.603	0.212	6
	$a^4P_{3/2}$	3133.482	31904.134	0.167	0.212	0.161	33
	$a^4P_{5/2}$	3165.443	31582.010	0.052	0.037	0.034	33
	$b^4P_{3/2}$	3343.811	29897.399	0.007	0.004	0.008	34
	$b^4P_{5/2}$	3369.261	29671.578	0.012	0.013	0.009	33
Residual				0.016			
$x^4D_{7/2}$	$a^4F_{7/2}$	2532.472	39475.240	0.063	0.062	0.025	32
τ = 2.4(1)ns[b]	$a^4F_{9/2}$	2568.871	38915.938	0.629	0.634	0.208	6
	$b^4F_{9/2}$	2740.347	36480.936	0.013	0.007	0.005	33
	$a^2F_{7/2}$	2960.242	33771.159	0.010	0.000	0.006	33
	$a^4P_{5/2}$	3106.576	32180.440	0.253	0.267	0.203	32
	$b^4P_{5/2}$	3302.649	30270.008	0.018	0.016	0.016	32
Residual				0.013			

[a] Biémont et al. (1981).
[b] Langhans et al. (1995).
[c] Sikström et al. (1999).
[d] Uncertainty in% in the f-value.
Note – Uncertainty in lifetime is given by figures in parentheses representing uncertainty in last figure(s).

Table 3. Zr II log gf-values. The lines are sorted by wavelength.

λ_{air} (Å)	λ_{vac} (Å)	χ_{exc} (eV)	Lower Level	Upper Level	log gf Exp.	Unc[a] (%)
2532.472	2533.233	0.095	$a^4F_{7/2}$	$x^4D_{7/2}$	−0.69	32
2542.112	2542.875	0.039	$a^4F_{5/2}$	$x^4D_{5/2}$	−0.64	33
2550.744	2551.510	0.000	$a^4F_{3/2}$	$x^4D_{3/2}$	−0.64	32
2567.637	2568.407	0.000	$a^4F_{3/2}$	$x^4D_{1/2}$	−0.17	4
2568.871	2569.641	0.164	$a^4F_{9/2}$	$x^4D_{7/2}$	+0.32	6
2571.391	2572.161	0.039	$a^4F_{5/2}$	$x^4D_{3/2}$	+0.04	8
2571.457	2572.228	0.095	$a^4F_{7/2}$	$x^4D_{5/2}$	+0.23	6
2639.080	2639.867	0.095	$a^4F_{7/2}$	$y^4F_{9/2}$	−0.67	21
2643.396	2644.184	0.039	$a^4F_{5/2}$	$z^4P_{3/2}$	−1.59	8
2667.793	2668.586	0.039	$a^4F_{5/2}$	$y^2F_{7/2}$	−0.86	11
2678.632	2679.428	0.164	$a^4F_{9/2}$	$y^4F_{9/2}$	+0.28	5
2693.524	2694.323	0.039	$a^4F_{5/2}$	$y^4F_{7/2}$	−0.98	9
2699.604	2700.405	0.039	$a^4F_{5/2}$	$y^2F_{5/2}$	−1.17	10
2700.130	2700.931	0.095	$a^4F_{7/2}$	$y^2F_{7/2}$	−0.08	6
2711.508	2712.312	0.000	$a^4F_{3/2}$	$y^4F_{5/2}$	−0.80	14
2712.419	2713.223	0.039	$a^4F_{5/2}$	$y^4D_{5/2}$	−0.99	9
2722.609	2723.416	0.164	$a^4F_{9/2}$	$y^4D_{7/2}$	+0.06	7
2726.491	2727.299	0.095	$a^4F_{7/2}$	$y^4F_{7/2}$	−0.22	7
2732.721	2733.530	0.095	$a^4F_{7/2}$	$y^2F_{5/2}$	−0.49	7
2734.851	2735.660	0.039	$a^4F_{5/2}$	$y^4F_{5/2}$	−0.06	6
2740.347	2741.158	0.466	$b^4F_{9/2}$	$x^4D_{7/2}$	−1.30	33
2741.547	2742.358	0.164	$a^4F_{9/2}$	$y^2F_{7/2}$	−0.90	11
2742.554	2743.365	0.000	$a^4F_{3/2}$	$y^4F_{3/2}$	−0.14	4
2745.854	2746.666	0.095	$a^4F_{7/2}$	$y^4D_{5/2}$	−0.31	6
2752.202	2753.015	0.039	$a^4F_{5/2}$	$y^4D_{3/2}$	−0.15	6
2758.806	2759.622	0.000	$a^4F_{3/2}$	$y^4D_{1/2}$	−0.56	7
2768.727	2769.545	0.164	$a^4F_{9/2}$	$y^4F_{7/2}$	−0.93	9
2865.605	2866.447	0.466	$b^4F_{9/2}$	$y^4F_{9/2}$	−1.27	21
2889.424	2890.271	0.319	$b^4F_{3/2}$	$y^4D_{5/2}$	−1.70	13
2898.712	2899.562	0.409	$b^4F_{7/2}$	$y^2F_{7/2}$	−1.22	11
2901.818	2902.668	0.359	$b^4F_{5/2}$	$y^2F_{5/2}$	−1.51	10
2915.993	2916.847	0.466	$b^4F_{9/2}$	$y^4D_{7/2}$	−0.50	11
2916.630	2917.484	0.359	$b^4F_{5/2}$	$y^4D_{5/2}$	−1.11	9
2934.611	2935.469	0.319	$b^4F_{3/2}$	$y^4D_{3/2}$	−0.98	12
2936.307	2937.166	0.409	$b^4F_{7/2}$	$y^2F_{5/2}$	−0.88	8
2951.475	2952.337	0.409	$b^4F_{7/2}$	$y^4D_{5/2}$	−0.77	8
2960.242	2961.107	0.802	$a^2F_{7/2}$	$x^4D_{7/2}$	−1.34	33
2962.679	2963.544	0.359	$b^4F_{5/2}$	$y^4D_{3/2}$	−0.57	12
2968.959	2969.826	0.466	$b^4F_{9/2}$	$y^4F_{7/2}$	−0.55	8
2969.623	2970.490	0.319	$b^4F_{3/2}$	$y^4D_{1/2}$	−0.70	10
2978.053	2978.922	0.409	$b^4F_{7/2}$	$y^4F_{5/2}$	−0.70	14
2979.180	2980.050	0.359	$b^4F_{5/2}$	$y^4F_{3/2}$	−0.85	17
2981.015	2981.885	0.559	$a^2D_{5/2}$	$y^4D_{7/2}$	−0.80	11
2990.129	2991.001	0.527	$a^2D_{3/2}$	$z^4S_{3/2}$	−1.85	12
3003.733	3004.609	0.559	$a^2D_{5/2}$	$y^2F_{7/2}$	−0.55	10
3013.323	3014.201	0.559	$a^2D_{5/2}$	$z^4S_{3/2}$	−1.28	8
3020.452	3021.331	0.527	$a^2D_{3/2}$	$y^2F_{5/2}$	−0.56	7
3030.919	3031.802	0.000	$a^4F_{3/2}$	$y^2D_{3/2}$	−1.04	4
3036.391	3037.275	0.559	$a^2D_{5/2}$	$y^4F_{7/2}$	−0.58	8
3036.503	3037.387	0.527	$a^2D_{3/2}$	$y^4D_{5/2}$	−0.96	9
3060.115	3061.005	0.039	$a^4F_{5/2}$	$y^2D_{3/2}$	−1.53	5
3060.425	3061.315	0.559	$a^2D_{5/2}$	$y^4D_{5/2}$	−0.79	8
3064.642	3065.533	0.527	$a^2D_{3/2}$	$y^4F_{5/2}$	−1.34	14
3065.207	3066.098	0.000	$a^4F_{3/2}$	$z^4D_{5/2}$	−1.97	8
3095.070	3095.969	0.039	$a^4F_{5/2}$	$z^4D_{5/2}$	−0.84	5
3099.228	3100.127	0.000	$a^4F_{3/2}$	$z^4D_{3/2}$	−0.96	7

Table 3. continued.

λ_{air} (Å)	λ_{vac} (Å)	χ_{exc} (eV)	Lower Level	Upper Level	log gf Exp.	Unc[a] (%)
3106.576	3107.478	0.999	$a^4P_{5/2}$	$x^4D_{7/2}$	+0.09	32
3110.874	3111.776	0.095	$a^4F_{7/2}$	$z^4D_{7/2}$	−0.90	5
3125.199	3126.105	0.527	$a^2D_{3/2}$	$y^4D_{1/2}$	−1.36	11
3125.919	3126.826	0.000	$a^4F_{3/2}$	$z^4D_{1/2}$	−0.70	5
3129.760	3130.668	0.039	$a^4F_{5/2}$	$z^4D_{3/2}$	−0.54	6
3133.482	3134.390	0.959	$a^4P_{3/2}$	$x^4D_{5/2}$	−0.19	33
3138.678	3139.588	0.095	$a^4F_{7/2}$	$z^4D_{5/2}$	−0.37	5
3155.676	3156.590	0.931	$a^4P_{1/2}$	$x^4D_{3/2}$	−0.57	33
3155.963	3156.877	0.713	$a^2F_{5/2}$	$y^4F_{7/2}$	−1.98	12
3156.994	3157.908	0.527	$a^2D_{3/2}$	$z^2P_{3/2}$	−0.93	10
3164.313	3165.229	0.713	$a^2F_{5/2}$	$y^2F_{5/2}$	−0.33	7
3165.443	3166.360	0.999	$a^4P_{5/2}$	$x^4D_{5/2}$	−0.69	33
3165.977	3166.894	0.164	$a^4F_{9/2}$	$z^4D_{7/2}$	−0.13	5
3166.265	3167.181	0.802	$a^2F_{7/2}$	$y^4D_{7/2}$	−0.51	11
3166.622	3167.538	0.758	$a^2P_{3/2}$	$z^4S_{3/2}$	−1.84	10
3178.086	3179.005	0.959	$a^4P_{3/2}$	$x^4D_{3/2}$	−0.62	33
3181.572	3182.492	0.931	$a^4P_{1/2}$	$x^4D_{1/2}$	−0.66	39
3181.935	3182.855	0.713	$a^2F_{5/2}$	$y^4D_{5/2}$	−0.75	8
3182.860	3183.781	0.559	$a^2D_{5/2}$	$z^2P_{3/2}$	+0.01	8
3191.905	3192.828	0.802	$a^2F_{7/2}$	$y^2F_{7/2}$	−0.52	10
3204.352	3205.278	0.959	$a^4P_{3/2}$	$x^4D_{1/2}$	−1.57	40
3208.313	3209.240	0.000	$a^4F_{3/2}$	$z^2D_{5/2}$	−1.97	7
3212.847	3213.775	0.713	$a^2F_{5/2}$	$y^4F_{5/2}$	−1.09	14
3214.189	3215.117	0.095	$a^4F_{7/2}$	$z^4F_{9/2}$	−0.40	7
3228.809	3229.741	0.802	$a^2F_{7/2}$	$y^4F_{7/2}$	−0.51	8
3231.692	3232.625	0.039	$a^4F_{5/2}$	$z^4F_{7/2}$	−0.47	7
3241.044	3241.980	0.039	$a^4F_{5/2}$	$z^2D_{5/2}$	−0.57	5
3256.526	3257.465	0.713	$a^2F_{5/2}$	$y^4F_{3/2}$	−2.01	19
3264.813	3265.754	0.931	$a^4P_{1/2}$	$z^4P_{3/2}$	−1.21	4
3273.047	3273.991	0.164	$a^4F_{9/2}$	$z^4F_{9/2}$	+0.30	5
3279.264	3280.209	0.095	$a^4F_{7/2}$	$z^4F_{7/2}$	+0.12	7
3284.712	3285.658	0.000	$a^4F_{3/2}$	$z^2D_{3/2}$	−0.37	5
3287.303	3288.250	0.319	$b^4F_{3/2}$	$y^2D_{3/2}$	−1.71	5
3288.374	3289.321	0.802	$a^2F_{7/2}$	$y^4F_{5/2}$	−1.97	16
3288.805	3289.752	0.959	$a^4P_{3/2}$	$z^4P_{3/2}$	−0.72	4
3302.649	3303.600	1.236	$b^4P_{5/2}$	$x^4D_{7/2}$	−1.01	32
3305.152	3306.104	0.039	$a^4F_{5/2}$	$z^2F_{7/2}$	−0.65	5
3309.891	3310.844	0.972	$a^2G_{7/2}$	$y^4D_{7/2}$	−1.26	12
3311.342	3312.295	0.710	$a^2P_{1/2}$	$z^2P_{3/2}$	−1.52	10
3313.700	3314.654	0.931	$a^4P_{1/2}$	$z^4S_{3/2}$	−0.87	7
3314.495	3315.449	0.713	$a^2F_{5/2}$	$z^2P_{3/2}$	−0.79	10
3318.512	3319.467	0.758	$a^2P_{3/2}$	$y^4D_{1/2}$	−1.15	11
3319.029	3319.984	0.039	$a^4F_{5/2}$	$z^2D_{3/2}$	−1.28	6
3334.253	3335.212	0.999	$a^4P_{5/2}$	$y^4D_{7/2}$	−0.35	11
3334.616	3335.575	0.559	$a^2D_{5/2}$	$z^2G_{7/2}$	−0.69	7
3337.921	3338.881	0.972	$a^2G_{7/2}$	$y^2F_{7/2}$	−1.54	11
3338.419	3339.379	0.959	$a^4P_{3/2}$	$z^4S_{3/2}$	−0.67	7
3340.553	3341.514	0.164	$a^4F_{9/2}$	$z^4F_{7/2}$	−0.57	7
3343.811	3344.773	1.208	$b^4P_{3/2}$	$x^4D_{5/2}$	−1.52	34
3344.786	3345.748	1.011	$a^2G_{9/2}$	$y^4D_{7/2}$	−0.35	11
3354.384	3355.348	0.758	$a^2P_{3/2}$	$z^2P_{3/2}$	−0.92	10
3357.261	3358.226	0.000	$a^4F_{3/2}$	$z^4F_{3/2}$	−0.66	5
3362.699	3363.665	0.999	$a^4P_{5/2}$	$y^2F_{7/2}$	−1.04	11
3363.811	3364.778	0.359	$b^4F_{5/2}$	$z^4D_{5/2}$	−1.24	5
3367.809	3368.776	0.319	$b^4F_{3/2}$	$z^4D_{3/2}$	−1.31	7
3369.261	3370.229	1.236	$b^4P_{5/2}$	$x^4D_{5/2}$	−1.28	33
3373.412	3374.381	1.011	$a^2G_{9/2}$	$y^2F_{7/2}$	−0.44	10

Table 3. continued.

λ_{air} (Å)	λ_{vac} (Å)	χ_{exc} (eV)	Lower Level	Upper Level	log gf Exp.	Unc^a (%)
3374.722	3375.692	0.999	$a^4P_{5/2}$	$z^4S_{3/2}$	−0.19	7
3376.262	3377.231	0.959	$a^4P_{3/2}$	$y^2F_{5/2}$	−0.86	7
3377.445	3378.415	0.409	$b^4F_{7/2}$	$z^4D_{7/2}$	−1.35	5
3378.299	3379.269	0.972	$a^2G_{7/2}$	$y^4F_{7/2}$	−1.33	9
3387.869	3388.841	0.972	$a^2G_{7/2}$	$y^2F_{5/2}$	−0.14	7
3388.200	3389.268	0.000	$a^4F_{3/2}$	$z^2F_{5/2}$	−0.41	3
3391.971	3392.945	0.164	$a^4F_{9/2}$	$z^4G_{11/2}$	+0.57	7
3393.119	3394.093	0.039	$a^4F_{5/2}$	$z^4F_{3/2}$	−0.74	6
3394.652	3395.627	1.208	$b^4P_{3/2}$	$x^4D_{3/2}$	−1.48	33
3396.330	3397.305	0.959	$a^4P_{3/2}$	$y^4D_{5/2}$	−0.63	8
3399.350	3400.326	0.319	$b^4F_{3/2}$	$z^4D_{1/2}$	−0.72	6
3403.682	3404.659	0.999	$a^4P_{5/2}$	$y^4F_{7/2}$	−0.60	8
3404.827	3405.804	0.359	$b^4F_{5/2}$	$z^4D_{3/2}$	−0.49	7
3408.076	3409.053	0.972	$a^2G_{7/2}$	$y^4D_{5/2}$	−0.66	8
3410.243	3411.222	0.409	$b^4F_{7/2}$	$z^4D_{5/2}$	−0.31	5
3413.397	3414.376	0.999	$a^4P_{5/2}$	$y^2F_{5/2}$	−1.14	8
3414.659	3415.638	1.011	$a^2G_{9/2}$	$y^4F_{7/2}$	−0.34	8
3419.106	3420.087	0.164	$a^4F_{9/2}$	$z^2F_{7/2}$	−1.65	6
3424.822	3425.804	0.039	$a^4F_{5/2}$	$z^2F_{5/2}$	−1.34	4
3430.527	3431.511	0.466	$b^4F_{9/2}$	$z^4D_{7/2}$	−0.16	5
3431.571	3432.555	0.959	$a^4P_{3/2}$	$y^4F_{5/2}$	−0.95	14
3432.404	3433.388	0.931	$a^4P_{1/2}$	$y^4D_{3/2}$	−0.72	12
3433.910	3434.895	0.999	$a^4P_{5/2}$	$y^4D_{5/2}$	−0.89	8
3438.231	3439.216	0.095	$a^4F_{7/2}$	$z^4G_{9/2}$	+0.41	3
3443.562	3444.549	0.972	$a^2G_{7/2}$	$y^4F_{5/2}$	−0.91	14
3454.572	3455.562	0.931	$a^4P_{1/2}$	$y^4F_{3/2}$	−1.33	17
3458.932	3459.923	0.959	$a^4P_{3/2}$	$y^4D_{3/2}$	−0.48	12
3469.940	3470.934	0.999	$a^4P_{5/2}$	$y^4F_{5/2}$	−1.36	14
3478.297	3479.293	0.095	$a^4F_{7/2}$	$z^2F_{5/2}$	−1.47	4
3479.017	3480.013	0.527	$a^2D_{3/2}$	$y^2D_{3/2}$	−0.67	4
3479.387	3480.383	0.713	$a^2F_{5/2}$	$z^2G_{7/2}$	+0.18	6
3480.398	3481.394	0.931	$a^4P_{1/2}$	$y^4D_{1/2}$	−0.78	11
3481.445	3482.442	0.959	$a^4P_{3/2}$	$y^4F_{3/2}$	−1.35	17
3496.205	3497.206	0.039	$a^4F_{5/2}$	$z^4G_{7/2}$	+0.26	5
3497.013	3498.014	0.319	$b^4F_{3/2}$	$z^2D_{5/2}$	−2.20	8
3497.893	3498.894	1.184	$b^4P_{1/2}$	$z^4P_{3/2}$	−1.54	5
3497.919	3498.920	0.999	$a^4P_{5/2}$	$y^4D_{3/2}$	−1.68	13
3499.571	3500.572	0.409	$b^4F_{7/2}$	$z^4F_{9/2}$	−1.06	7
3505.666	3506.669	0.164	$a^4F_{9/2}$	$z^4G_{9/2}$	−0.39	8
3507.677	3508.680	0.959	$a^4P_{3/2}$	$y^4D_{1/2}$	−1.42	11
3510.455	3511.459	0.559	$a^2D_{5/2}$	$y^2D_{3/2}$	−1.04	5
3520.874	3521.881	0.559	$a^2D_{5/2}$	$z^4D_{7/2}$	−1.29	5
3521.274	3522.281	1.208	$b^4P_{3/2}$	$z^4P_{3/2}$	−1.39	5
3525.807	3526.815	0.359	$b^4F_{5/2}$	$z^4F_{7/2}$	−0.96	7
3536.943	3537.954	0.359	$b^4F_{5/2}$	$z^2D_{5/2}$	−1.41	6
3549.508	3550.522	1.236	$b^4P_{5/2}$	$z^4P_{3/2}$	−0.72	4
3551.951	3552.966	0.095	$a^4F_{7/2}$	$z^4G_{7/2}$	−0.36	8
3554.071	3555.086	1.184	$b^4P_{1/2}$	$z^4S_{3/2}$	−0.81	7
3556.594	3557.610	0.466	$b^4F_{9/2}$	$z^4F_{9/2}$	+0.07	6
3568.137	3569.156	0.802	$a^2F_{7/2}$	$z^2G_{7/2}$	−1.33	7
3569.316	3570.335	0.527	$a^2D_{3/2}$	$z^4D_{3/2}$	−2.27	10
3572.468	3573.488	0.000	$a^4F_{3/2}$	$z^4G_{5/2}$	+0.03	5
3576.853	3577.874	0.409	$b^4F_{7/2}$	$z^4F_{7/2}$	−0.12	7
3578.211	3579.233	1.208	$b^4P_{3/2}$	$z^4S_{3/2}$	−0.66	7
3587.974	3588.998	0.319	$b^4F_{3/2}$	$z^2D_{3/2}$	−0.80	6
3588.314	3589.338	0.409	$b^4F_{7/2}$	$z^2D_{5/2}$	−1.13	5
3588.806	3589.831	0.999	$a^4P_{5/2}$	$z^2P_{3/2}$	−1.81	11

Table 3. continued.

$\lambda_{\rm air}$ (Å)	$\lambda_{\rm vac}$ (Å)	$\chi_{\rm exc}$ (eV)	Lower Level	Upper Level	log gf Exp.	Unc[a] (%)
3607.369	3608.398	1.236	$b^4P_{5/2}$	$z^4S_{3/2}$	−0.70	7
3613.098	3614.128	0.039	$a^4F_{5/2}$	$z^4G_{5/2}$	−0.58	8
3630.020	3631.055	0.359	$b^4F_{5/2}$	$z^2D_{3/2}$	−1.11	6
3636.444	3637.481	0.466	$b^4F_{9/2}$	$z^4F_{7/2}$	−1.24	7
3667.062	3668.106	0.409	$b^4F_{7/2}$	$z^2F_{7/2}$	−2.15	7
3671.264	3672.310	0.713	$a^2F_{5/2}$	$y^2D_{3/2}$	−0.58	5
3672.664	3673.710	0.095	$a^4F_{7/2}$	$z^4G_{5/2}$	−2.21	7
3674.714	3675.761	0.319	$b^4F_{3/2}$	$z^4F_{3/2}$	−0.51	6
3697.457	3698.510	0.466	$b^4F_{9/2}$	$z^4G_{11/2}$	−0.78	10
3714.777	3715.834	0.527	$a^2D_{3/2}$	$z^2D_{5/2}$	−0.96	5
3718.830	3719.888	0.359	$b^4F_{5/2}$	$z^4F_{3/2}$	−1.76	6
3721.690	3722.748	0.713	$a^2F_{5/2}$	$z^4D_{5/2}$	−2.42	10
3729.722	3730.783	0.466	$b^4F_{9/2}$	$z^2F_{7/2}$	−1.56	5
3738.123	3739.186	0.559	$a^2D_{5/2}$	$z^4F_{7/2}$	−1.84	8
3750.642	3751.708	0.559	$a^2D_{5/2}$	$z^2D_{5/2}$	−1.45	6
3751.590	3752.656	0.972	$a^2G_{7/2}$	$z^2G_{7/2}$	+0.00	7
3766.815	3767.885	0.409	$b^4F_{7/2}$	$z^4G_{9/2}$	−0.83	7
3767.879	3768.950	0.710	$a^2P_{1/2}$	$z^4D_{3/2}$	−1.75	7
3771.962	3773.033	0.713	$a^2F_{5/2}$	$z^4D_{3/2}$	−2.22	9
3772.056	3773.127	0.758	$a^2P_{3/2}$	$z^4D_{5/2}$	−1.63	6
3782.232	3783.307	0.802	$a^2F_{7/2}$	$z^4D_{7/2}$	−1.84	6
3796.482	3797.560	1.011	$a^2G_{9/2}$	$z^2G_{7/2}$	−0.89	7
3807.403	3808.484	0.710	$a^2P_{1/2}$	$z^4D_{1/2}$	−2.30	11
3814.958	3816.041	0.409	$b^4F_{7/2}$	$z^2F_{5/2}$	−2.26	6
3817.585	3818.669	0.527	$a^2D_{3/2}$	$z^2D_{3/2}$	−1.13	6
3819.814	3820.898	1.208	$b^4P_{3/2}$	$z^2P_{3/2}$	−2.35	15
3823.411	3824.496	0.802	$a^2F_{7/2}$	$z^4D_{5/2}$	−2.07	7
3836.761	3837.849	0.559	$a^2D_{5/2}$	$z^2F_{7/2}$	−0.12	5
3843.018	3844.109	0.359	$b^4F_{5/2}$	$z^4G_{7/2}$	−0.94	7
3853.061	3854.153	1.236	$b^4P_{5/2}$	$z^2P_{3/2}$	−1.91	11
3915.934	3917.043	0.527	$a^2D_{3/2}$	$z^4F_{3/2}$	−0.85	6
3934.114	3935.227	0.319	$b^4F_{3/2}$	$z^4G_{5/2}$	−1.08	6
3934.785	3935.899	0.713	$a^2F_{5/2}$	$z^2D_{5/2}$	−0.91	5
3936.051	3937.165	0.802	$a^2F_{7/2}$	$z^4F_{9/2}$	−1.58	7
3958.220	3959.340	0.527	$a^2D_{3/2}$	$z^2F_{5/2}$	−0.32	4
3991.127	3992.256	0.758	$a^2P_{3/2}$	$z^2D_{5/2}$	−0.31	5
3998.965	4000.095	0.559	$a^2D_{5/2}$	$z^2F_{5/2}$	−0.52	4
4018.377	4019.512	0.959	$a^4P_{3/2}$	$z^4D_{5/2}$	−1.27	5
4024.435	4025.573	0.999	$a^4P_{5/2}$	$z^4D_{7/2}$	−1.13	5
4029.675	4030.813	0.713	$a^2F_{5/2}$	$z^2F_{7/2}$	−0.78	5
4034.083	4035.223	0.802	$a^2F_{7/2}$	$z^4F_{7/2}$	−1.51	8
4040.240	4041.382	0.931	$a^4P_{1/2}$	$z^4D_{3/2}$	−1.65	7
4045.613	4046.756	0.710	$a^2P_{1/2}$	$z^2D_{3/2}$	−0.86	6
4048.666	4049.810	0.802	$a^2F_{7/2}$	$z^2D_{5/2}$	−0.53	5
4050.320	4051.464	0.713	$a^2F_{5/2}$	$z^2D_{3/2}$	−1.06	6
4071.089	4072.239	0.999	$a^4P_{5/2}$	$z^4D_{5/2}$	−1.66	6
4077.046	4078.197	0.959	$a^4P_{3/2}$	$z^4D_{3/2}$	−1.69	7
4085.719	4086.873	0.931	$a^4P_{1/2}$	$z^4D_{1/2}$	−1.84	49
4096.628	4097.784	0.559	$a^2D_{5/2}$	$z^4G_{7/2}$	−1.73	8
4149.198	4150.368	0.802	$a^2F_{7/2}$	$z^2F_{7/2}$	−0.04	5
4156.232	4157.404	0.710	$a^2P_{1/2}$	$z^4F_{3/2}$	−0.78	6
4161.200	4162.373	0.713	$a^2F_{5/2}$	$z^4F_{3/2}$	−0.59	6
4179.808	4180.987	1.665	$b^2D_{3/2}$	$y^2F_{5/2}$	−0.68	8
4186.682	4187.862	1.756	$b^2D_{5/2}$	$y^4D_{7/2}$	−0.74	11
4191.493	4192.675	1.759	$b^2G_{9/2}$	$y^4D_{7/2}$	−1.07	11
4208.980	4210.166	0.713	$a^2F_{5/2}$	$z^2F_{5/2}$	−0.51	4
4210.609	4211.795	1.665	$b^2D_{3/2}$	$y^4D_{5/2}$	−1.19	9

Table 3. continued.

$\lambda_{\rm air}$ (Å)	$\lambda_{\rm vac}$ (Å)	$\chi_{\rm exc}$ (eV)	Lower Level	Upper Level	log gf Exp.	Unc[a] (%)
4211.877	4213.063	0.527	$\mathrm{a^2D_{3/2}}$	$\mathrm{z^4G_{5/2}}$	−1.04	6
4224.264	4225.454	0.758	$\mathrm{a^2P_{3/2}}$	$\mathrm{z^4F_{3/2}}$	−1.88	6
4231.629	4232.821	1.756	$\mathrm{b^2D_{5/2}}$	$\mathrm{y^2F_{7/2}}$	−0.79	10
4258.041	4259.240	0.559	$\mathrm{a^2D_{5/2}}$	$\mathrm{z^4G_{5/2}}$	−1.20	6
4264.908	4266.109	1.665	$\mathrm{b^2D_{3/2}}$	$\mathrm{y^4F_{5/2}}$	−1.63	14
4272.251	4273.454	1.827	$\mathrm{c^2D_{5/2}}$	$\mathrm{z^4P_{3/2}}$	−0.95	4
4273.513	4274.715	0.758	$\mathrm{a^2P_{3/2}}$	$\mathrm{z^2F_{5/2}}$	−1.48	4
4286.503	4287.709	0.972	$\mathrm{a^2G_{7/2}}$	$\mathrm{z^2D_{5/2}}$	−1.61	6
4289.152	4290.359	1.827	$\mathrm{c^2D_{5/2}}$	$\mathrm{y^4D_{7/2}}$	−1.68	16
4293.125	4294.333	1.743	$\mathrm{b^2G_{7/2}}$	$\mathrm{y^2F_{5/2}}$	−1.01	8
4296.733	4297.942	1.756	$\mathrm{b^2D_{5/2}}$	$\mathrm{y^4F_{7/2}}$	−1.01	8
4301.801	4303.011	1.759	$\mathrm{b^2G_{9/2}}$	$\mathrm{y^4F_{7/2}}$	−1.20	9
4312.225	4313.438	1.756	$\mathrm{b^2D_{5/2}}$	$\mathrm{y^2F_{5/2}}$	−1.59	10
4317.309	4318.524	0.713	$\mathrm{a^2F_{5/2}}$	$\mathrm{z^4G_{7/2}}$	−1.45	8
4336.338	4337.558	1.827	$\mathrm{c^2D_{5/2}}$	$\mathrm{y^2F_{7/2}}$	−1.75	13
4337.619	4338.838	1.773	$\mathrm{c^2D_{3/2}}$	$\mathrm{y^2F_{5/2}}$	−1.22	8
4339.549	4340.769	0.802	$\mathrm{a^2F_{7/2}}$	$\mathrm{z^2F_{5/2}}$	−1.99	5
4359.730	4360.956	1.236	$\mathrm{b^4P_{5/2}}$	$\mathrm{z^4D_{7/2}}$	−0.51	5
4370.948	4372.176	1.208	$\mathrm{b^4P_{3/2}}$	$\mathrm{z^4D_{5/2}}$	−0.77	5
4403.338	4404.575	1.184	$\mathrm{b^4P_{1/2}}$	$\mathrm{z^4D_{3/2}}$	−1.18	7
4404.730	4405.968	1.827	$\mathrm{c^2D_{5/2}}$	$\mathrm{y^4F_{7/2}}$	−1.68	11
4414.535	4415.775	1.236	$\mathrm{b^4P_{5/2}}$	$\mathrm{z^4D_{5/2}}$	−1.08	5
4440.453	4441.700	1.208	$\mathrm{b^4P_{3/2}}$	$\mathrm{z^4D_{3/2}}$	−1.04	7
4442.500	4443.748	0.999	$\mathrm{a^4P_{5/2}}$	$\mathrm{z^2F_{7/2}}$	−1.94	7
4442.992	4444.239	1.486	$\mathrm{a^2H_{9/2}}$	$\mathrm{z^2G_{7/2}}$	−0.42	7
4454.795	4456.046	0.802	$\mathrm{a^2F_{7/2}}$	$\mathrm{z^4G_{7/2}}$	−1.18	7
4457.413	4458.664	1.184	$\mathrm{b^4P_{1/2}}$	$\mathrm{z^4D_{1/2}}$	−1.22	6
4461.217	4462.469	1.011	$\mathrm{a^2G_{9/2}}$	$\mathrm{z^2F_{7/2}}$	−1.13	5
4485.444	4486.703	1.236	$\mathrm{b^4P_{5/2}}$	$\mathrm{z^4D_{3/2}}$	−2.01	9
4495.449	4496.711	1.208	$\mathrm{b^4P_{3/2}}$	$\mathrm{z^4D_{1/2}}$	−1.83	7
4496.962	4498.224	0.713	$\mathrm{a^2F_{5/2}}$	$\mathrm{z^4G_{5/2}}$	−0.89	6
4613.946	4615.238	0.972	$\mathrm{a^2G_{7/2}}$	$\mathrm{z^2F_{5/2}}$	−1.54	5
4831.327	4832.677	1.208	$\mathrm{b^4P_{3/2}}$	$\mathrm{z^2D_{3/2}}$	−1.72	7
5112.270	5113.695	1.665	$\mathrm{b^2D_{3/2}}$	$\mathrm{y^2D_{3/2}}$	−0.85	5
5350.350	5351.836	1.773	$\mathrm{c^2D_{3/2}}$	$\mathrm{y^2D_{3/2}}$	−1.16	5
5372.466	5373.960	2.409	$\mathrm{b^2F_{7/2}}$	$\mathrm{y^4D_{7/2}}$	−0.81	12

[a] Uncertainty in% in the f-value.